Photoemission studies of the Na/Ge(111)-3 × 1 surface

1998 J. Phys.: Condens. Matter 10 3731

(http://iopscience.iop.org/0953-8984/10/17/006)

J. Phys.: Condens. Matter **10** (1998) 3731–3741. Printed in the UK PII: S0953-8984(98)86003-7

Photoemission studies of the Na/Ge(111)–3 × 1 surface

Jeong Won Kim†, Sehun Kim†, Jae Myung Seo‡, Shin-ichiro Tanaka§ and Masao Kamada§

† Department of Chemistry and Centre for Molecular Science, Korea Advanced Institute of Science and Technology, Taejon 305-701, Korea

‡ Department of Physics, Jeonbuk National University, Jeonju 560-756, Korea

§ UVSOR, Institute for Molecular Science, Myodaiji, Okazaki 444, Japan

Received 14 July 1997, in final form 2 December 1997

Abstract. The electronic structure of a Na/Ge(111)–3 × 1 surface was investigated by valence-band and core-level photoemission spectroscopy with synchrotron radiation. The two-dimensional energy-band dispersion of the surface Brillouin zone along $\overline{\mathrm{M}}$–$\overline{\Gamma}$–$\overline{\mathrm{K}}$ was mapped out. The experimental surface-state dispersions show a better agreement with the theoretical results for the buckled Seiwatz model than the extended Pandey model. The surface core-level shift of the (3 × 1) surface is explained on the basis of the buckled Seiwatz model. The (3 × 1) surface reveals more covalent bonding character than other Na-adsorbed surfaces at room temperature, and its surface Fermi level is close to the valence-band maximum.

1. Introduction

The electronic and atomic structure of alkali metals (AMs) on semiconductor surfaces has been of great interest in the past few decades due to their important applications in science and technology. Because of its single-valence-electron configuration, the AM overlayer on a semiconductor has become an active research area as a simple model system exhibiting Schottky barrier formation and metallization [1]. However, there are many interesting and unsolved problems relating to the AM/semiconductor surface itself. It is well known that adsorption of submonolayer of AM on a semiconductor surface reduces the work function and enhances the oxidation. As an example of initial-stage phenomena, the AM-induced (3 × 1) reconstruction, first observed by Daimon and Ino [2], exhibits many interesting characteristics such as semiconducting and passivating natures [3–5]. The (3 × 1) surface seems to have a universal structure, irrespective of the adsorbate species [6]. However, the atomic and electronic structures of the AM-induced (3 × 1) surfaces have remained unresolved [3–17].

Several structural models for the (3 × 1) reconstruction of AM/Si(111) have been proposed experimentally [3, 5, 6, 9, 11, 12] and theoretically [13–15]. Recently, on the basis of the absolute AM coverage of a third of a monolayer (ML), the favourable candidates have been narrowed down to two models: the buckled Seiwatz (missing-top-layer) model with Peierls-like distortion of the Si chain and the extended Pandey model with the buckled π-bonded-chain structure. Figure 1 shows the two models. In the buckled Seiwatz model, five-membered Si rings form a π-chain, whose empty channel is occupied with 1/3 ML of AM adsorbate on the threefold site. The AM bonding and structural instability induce the buckling of the π-chain, gaining a large band-energy stabilization. The extended Pandey

0953-8984/98/173731+11$19.50

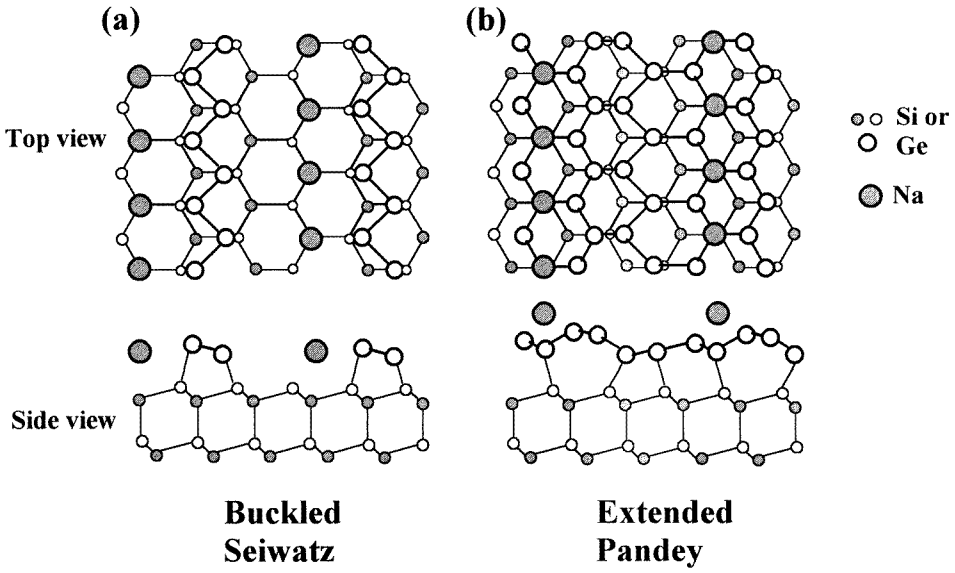

Figure 1. Geometrical models of (a) the buckled Seiwatz model and (b) the extended Pandey model for the AM-induced (3×1) surface [14–16]. Small circles indicate the subsurface atoms and large circles indicate the top-layer substrate atoms. Large shaded circles indicate the AM atoms.

model consists of 7–5–6-membered rings as the top Si surface geometry. It resembles the π-bonded chain model proposed for the cleaved Si(111)–2×1 surface [18]. In this model, the AM is adsorbed on the reconstructed Si substrate. The total energy calculation results slightly favoured the extended Pandey model over the Seiwatz model [14]. However, the total energy difference between the two models appears negligibly small [15]. The surface-state dispersion determined by the angle-resolved photoemission spectroscopy (ARPES) measurement was in partial agreement with estimation of the Seiwatz model in the surface Brillouin zone (SBZ) [9, 15, 16].

The surface atomic and electronic structure of Na/Ge(111)–3×1 is expected to be similar to that of Si(111) [17]. Despite their similarities as regards the surface periodicity and passivating properties, most of the studies have been conducted on the AM/Si(111) system, rather than on Ge. As a starting surface, the simple adatom structure of Ge(111)–c(2×8) makes it easier to investigate the (3×1) transition, and might produce complementary information about the (3×1) surface. In this article, the surface electronic properties of Na/Ge(111)–3×1 are studied using ARPES and surface-sensitive core-level spectroscopy based on synchrotron radiation. In addition, the ARPES data are compared with the recent first-principles calculations for the buckled Seiwatz model and the extended Pandey model.

2. Experimental procedure

The experiments were carried out at beam line BL6A2 of UVSOR at the Institute for Molecular Science in Okazaki, Japan [19]. Synchrotron radiation from the 750 MeV storage ring was dispersed by a plane grating monochromator covering the photon energy range $h\nu = 10$–130 eV. The ultrahigh-vacuum chamber (base pressure: 2×10^{-10} Torr) was equipped with a rear-view low-energy electron diffraction (LEED) optics, a cylindrical

mirror analyser for Auger electron spectroscopy (AES), and a hemispherical analyser having an angular resolution of $\pm 1^{\circ}$. During the photoemission measurement the overall energy resolution was 0.15–0.20 eV.

The p-type Ge(111) wafer (B-doped, $\rho \sim 10\ \Omega$ cm) was cleaned by means of repeated cycles of Ar^{+} sputtering ($E = 1$ keV, $I = 1.0\ \mu$A) and annealing ($T \simeq 700\ ^{\circ}$C). After the cleaning procedure, a distinct c(2 × 8) LEED pattern was observed, and impurities such as C and O were not detected in the AES spectrum. Na was evaporated on the room temperature (RT) substrate by a well outgassed dispenser cell (SAES Getters Incorporated) positioned at 5 cm away from the sample. After the deposition of Na, LEED showed a diffuse (1 × 1) pattern, and the subsequent flashing to 400 °C for about ten seconds resulted in a three-domain (3 × 1) pattern. This (3 × 1) reconstruction did not critically depend upon the amount of Na initially deposited. This must be because the unreacted Na atoms desorb with post-annealing at 400 °C. Upon additional annealing at 700 °C for five minutes, a well ordered c(2 × 8) periodicity of the clean surface was recovered. The work-function change ($\Delta\phi$) with the Na deposition was measured from the secondary-electron cut-off energy in the photoelectron spectrum obtained from the sample with −10 V bias voltage. The Na coverage was determined by the core-level intensity ratio of the Na 2p level to the Ge 3d level (±20% error), taking into consideration the photoionization cross section of these levels [20]. 1 ML is defined as 7.22×10^{14} atoms cm^{-2}.

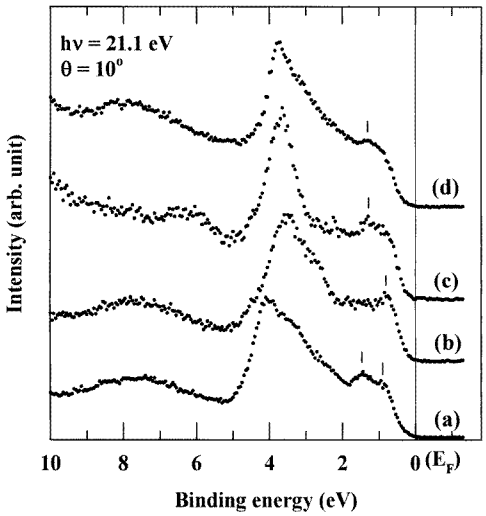

Figure 2. Valence-band spectra for (a) clean Ge(111)–c(2 × 8), (b) 0.16 ML Na on Ge(111), (c) 1.0 ML Na/Ge(111), and (d) Na/Ge(111)–3 × 1 surfaces at $h\nu = 21.1$ eV.

3. Results and discussion

3.1. Angle-resolved photoemission spectra

Figure 2 shows valence-band spectra for the photon energy $h\nu = 21.1$ eV for (a) clean Ge(111)–c(2×8), (b) 0.16 ML Na on Ge(111), (c) 1.0 ML Na/Ge(111), and (d) Na/Ge(111)–3 × 1 surfaces. The photon angle of incidence was 45° from the surface normal and the emission angle of the photoelectrons was set to 10° (the $[1\bar{1}0]$ direction) at which a maximum

counting rate was observed. The binding energies (E_bs) are referred to the Fermi level (E_F) determined by the sharp decreasing edge in the photoemission spectra of thick Au film deposited on the sample. In addition to the main bulk peak at $E_b = 4$ eV, the spectrum of clean Ge(111)–c(2×8) clearly shows two surface states, a rest-atom dangling-bond state at about $E_b = 0.9$ eV and an adatom back-bond state at $E_b = 1.4$ eV, which are already known of [21–23]. After Na evaporation, two surface-state peaks appear to merge as a single peak at $E_b = 0.8$ eV in figure 2(b) and at $E_b = 1.3$ eV in figure 2(c). This Na-induced change in the valence-band spectra is the same as was reported before [10, 24, 25]. For the (3×1) surface in figure 2(d), the single broad peak at about $E_b = 1.3$ eV is attributed to a modified surface state induced by Na [10]. The valence-band spectra also show that the clean and other Na/Ge(111) surfaces are all semiconducting because there is no emission intensity near E_F.

In figure 3, ARPES spectra for $h\nu = 21.1$ eV are shown for the Na/Ge(111)–3×1 surface as a function of the emission angle θ measured away from the normal to the surface: in figure 3(a), those for the $\overline{\Gamma}$–$\overline{K}$ [$1\bar{1}0$] direction of the (1×1) SBZ shown in

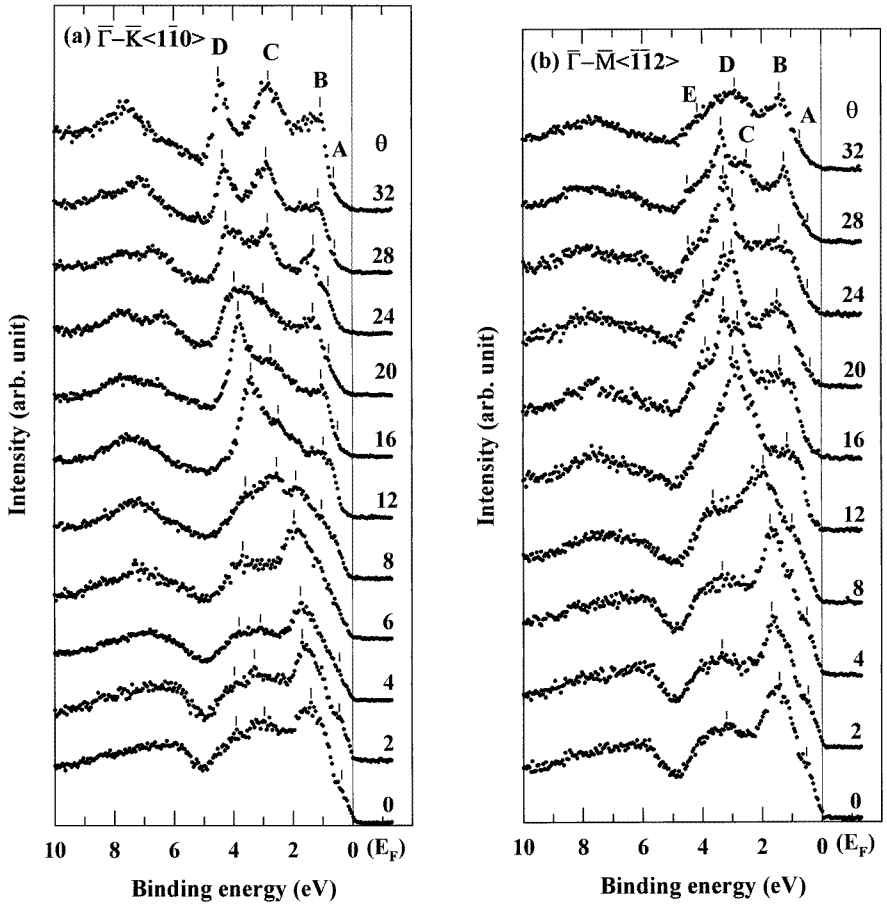

Figure 3. ARPES spectra of a Na/Ge(111)–3×1 surface for a series of polar angles θ (a) along the $\overline{\Gamma}$–$\overline{K}$ [$1\bar{1}0$] direction and (b) along the $\overline{\Gamma}$–$\overline{M}$ [$\bar{1}\bar{1}2$] direction of the (1×1) SBZ at $h\nu = 21.1$ eV.

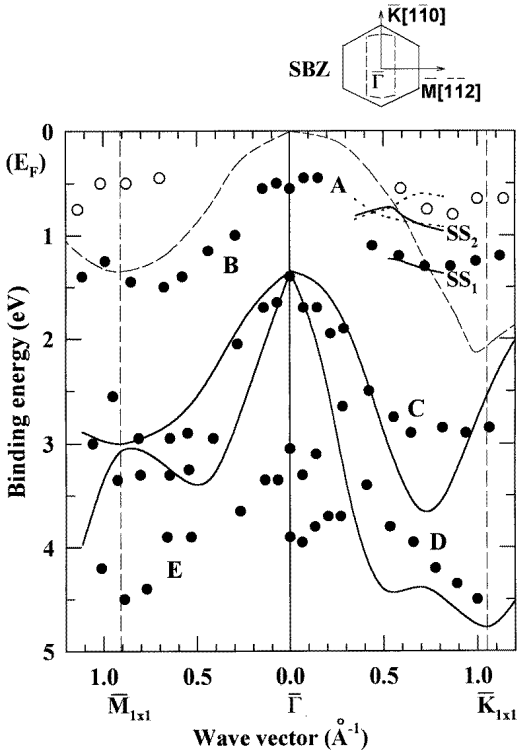

Figure 4. The experimental energy-band dispersion (closed circles) for Na/Ge(111)–3 × 1 at $h\nu = 21.1$ eV: a plot of E_b versus the momentum parallel to the surface, i.e., the $\overline{\Gamma}$–$\overline{M}$ and the $\overline{\Gamma}$–$\overline{K}$ azimuth directions. Open circles indicate weak peaks. The solid curves show the results of the theoretical band calculations for bulk Ge and the dashed curve shows the projected bulk valence-band maximum [26]. In part of the $\overline{\Gamma}$–$\overline{K}$ SBZ, the surface bands SS_1 and SS_2 are shown as solid lines for the buckled Seiwatz model and dotted lines for the extended Pandey model, as calculated using an *ab initio* pseudopotential density-functional scheme [31].

figure 4; and in figure 3(b), those for the $\overline{\Gamma}$–$\overline{M}$ [$\bar{1}\bar{1}$2] direction. Both sets of spectra commonly demonstrate two surface-state features modified from the clean surface by Na deposition. The weak feature A is visible as a shoulder at $E_b \simeq 0.5$ eV below E_F. The feature B appears distinctly at $E_b = 1.0$–1.5 eV for emission angles larger than $\theta = 12^\circ$. Its intensity is pronounced near the SBZ boundary for both directions. Both features show a slight dispersion with the increment of the emission angle, but appear at the same binding energies in the normal-emission spectra at different photon energies ($h\nu = 18$–34 eV, not shown here). The remaining features are similar to the bulk peaks observed for the clean c(2 × 8) surface. In both directions, two highly dispersive bulk bands (C and D) cannot be resolved near the centre of the SBZ, but begin to split from $\theta = 12^\circ$. Other nondispersive structures near 4 eV and 7 eV around the centre of the SBZ are manifestations of the three-dimensional densities of states at the critical points [26–28]. Another feature, E, is weak but dispersive from 4.2 eV at $\theta = 32^\circ$ via 4.5 eV at $\theta = 28^\circ$ and back to 3.9 eV at $\theta = 16^\circ$ in figure 3(b). It is not a direct transition, but seems to be a secondary emission originating from another core level [27].

In figure 4, the energy-band dispersion (circular symbols) obtained from the ARPES data for Na/Ge(111)–3 × 1 is presented along the $\overline{M}$–$\overline{\Gamma}$–$\overline{K}$ direction of the (1 × 1) SBZ. We

apply a free-electron approximation for the final-state dispersion. The band mapping was followed using the formula $k_{\parallel} = (1/\hbar)\sqrt{2m(h\nu - \phi - E_b)}\sin\theta$, where $k_{\parallel}$ is the component of the wave vector parallel to the surface, $h\nu = 21.1$ eV, and ϕ the work function (3.75 eV). The high-binding-energy bulk bands ($E_b \geqslant 5$ eV) are excluded for simplicity. The dashed line shows the projected bulk-band maximum. The solid curves present the theoretical bulk energy band [26] which is in good agreement with the experimental dispersion (C and D). In addition, the theoretical surface-state bands (SS_1 and SS_2) for the buckled Seiwatz model (solid lines) and the extended Pandey model (dotted lines) are presented, which are only available along $\overline{\Gamma}$–$\overline{K}$ [31]. Jeong and Kang used the norm-conserving separable pseudopotentials together with the density-functional theory within the local-density approximation (LDA). They simulated the AM/Ge(111) surface by a periodic slab geometry with a substrate of twelve Ge layers and a vacuum layer equivalent to six Ge layers. The positions of the surface bands and their dispersions indicated by the present experimental data (A and B) are in better agreement with the buckled Seiwatz model than with the extended Pandey model. The total energy calculation for Na/Ge(111)–3×1 also slightly favours the buckled Seiwatz model over the extended Pandey model by ~0.03 eV/cell [31]. Hence, for the (3×1) reconstruction of Na/Ge(111), both the ARPES results and the total energy calculation favour the buckled Seiwatz model. This result is contrary to the case for AM/Si(111)–3×1, for which the ARPES results are consistent with the calculated band structure for the Seiwatz model, but the total energy calculations favour the extended Pandey model. According to Weitering *et al*, the discrepancy between the theory and experiment may indicate that exchange and correlation in π-bonded Si chains should be given more consideration, beyond the mean-field band-structure approach [16].

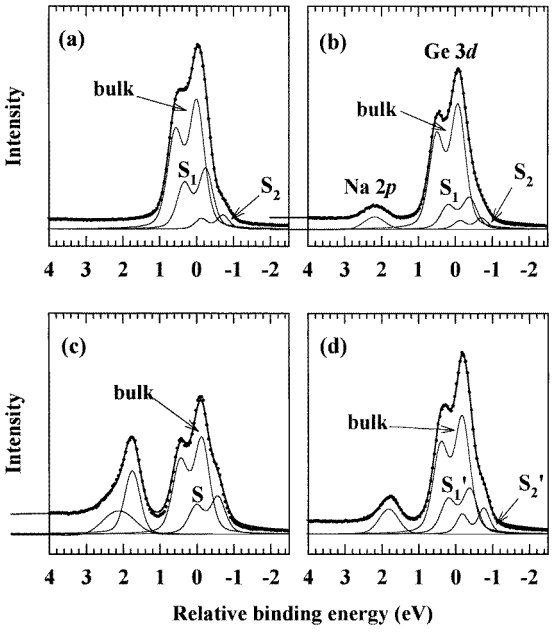

Figure 5. Core-level spectra and fitting results for (a) clean Ge(111)–c(2×8), (b) 0.16 ML Na on Ge(111)–c(2×8), (c) 1.0 ML Na/Ge(111), and (d) Na/Ge(111)–3×1 surfaces. The fitting parameters are listed in table 1.

Table 1. Fitting parameters for the components used to fit the Ge 3d core-level spectra shown in figure 5. All of the energies are in eV. The Lorentzian and Gaussian widths refer to the full width at half-maximum. The intensity ratio R is defined as the area of the surface component/total area of Ge 3d core level. (The branching ratio = 0.754, the Lorentzian width = 0.150, and the spin–orbit splitting = 0.585.)

	Ge(111)–c(2 × 8)	Na/Ge(111)	Na/Ge(111)	Na/Ge(111)–3 × 1
Na coverage (ML)	0	0.16	1.0	0.26
Bulk component				
Gaussian width	0.40	0.39	0.39	0.40
Surface component	S_1	S_1	S	S_1'
Core-level shift	−0.25	−0.31	−0.43	−0.20
Gaussian width	0.37	0.38	0.37	0.39
Intensity ratio R	0.292	0.193	0.279	0.247
Surface component	S_2	S_2		S_2'
Core-level shift	−0.71	−0.63		−0.58
Gaussian width	0.30	0.29		0.27
Intensity ratio R	0.061	0.059		0.111

3.2. Core-level analysis

Figure 5 shows Na 2p and Ge 3d core-level spectra obtained from (a) clean Ge(111)–c(2×8), (b) 0.16 ML Na on Ge(111), (c) 1.0 ML Na/Ge(111), and (d) Na/Ge(111)–3 × 1 surfaces. The photon energy of 74 eV was chosen in order to enhance the surface sensitivity. The relative binding energy is referred to the bulk Ge $3d_{5/2}$ level of clean Ge(111) [32]. In order to fit the core-level spectra, a nonlinear least-squares routine [33] was used after subtraction of the cubic polynomial background. The fitting parameters and the results for the Ge 3d level are listed in table 1.

As shown in figure 5(a), the clean Ge(111)–c(2 × 8) has two surface components at −0.25 eV (S_1) and −0.71 eV (S_2) relative to the bulk, and the intensity ratio of S_2/S_1 is 0.21; these values are well matched with the previous results [34, 35]. Most of the previous results have explained the structure of Ge(111)–c(2 × 8) on the basis of the rest-atom–adatom model [23, 36, 37]. In particular, the STM studies and the theoretical calculations reported that there are some degrees of charge transfer from the adatom to the rest atom [23, 37]. Since the excess charge at the rest atoms results in a lower binding-energy shift of the core level, the lower-binding-energy surface component S_2 on Ge(111)–c(2 × 8) in figure 5(a) was ascribed to the rest atoms [38]. The other component, S_1, was attributed to the adatoms and their back-bonding atoms [39]. On the basis of this simple rest-atom–adatom structural model for clean Ge(111)–c(2 × 8), the intensity ratio sum (35%) of these surface components, S_1 (29%) and S_2 (6%), almost represents the intensity of the surface Ge atoms in a c(2×8) unit mesh (four adatoms, twelve back-bonding first-layer atoms, and four rest atoms). Although Göthelid *et al* reported that there is another surface component [39], we take into account only two surface components due to the relatively low resolution of our spectrometer. In this assignment, the Ge atoms below the second layer were considered as bulk atoms.

Figures 5(b) and 5(c) show the core-level spectra and deconvoluted results for 0.16 ML Na/Ge(111) and 1.0 ML Na/Ge(111) surfaces. The position of the lower-binding-energy peak (S_2) is shifted toward higher binding energy, and finally the peaks merge into a single

peak (S) as the Na coverage increases. We note also that the intensity of the shoulder at low binding energy grows roughly proportionally to the Na coverage, like in the case of K/Si(111) surfaces [24, 40]. Therefore, the lower-binding-energy surface component (S_2 in figure 5(b) and S in figure 5(c)) is attributed to the Ge atoms adjacent to Na atoms, and the other higher-binding-energy component (S_1 in figure 5(b)) to the bare Ge surface.

Figure 5(d) shows the Ge 3d and Na 2p core-level spectra for Na/Ge(111)–3×1. There are two surface components at lower binding energies, -0.20 eV (S'_1) and -0.58 eV (S'_2), which are very similar to those in a previous report on K/Ge(111) surfaces [41]. A single Na 2p peak appears at 1.95 eV higher binding energy than the bulk Ge $3d_{5/2}$ peak. Since the photoionization cross sections of Na 2p and Ge 3d are almost the same (7 Mb) for 74 eV photons [20], the number of Na atoms in a (3×1) unit mesh can be estimated by comparing the intensity of the Na peak with that of surface Ge peaks. The intensity ratios of S'_1, S'_2, and Na 2p are 25%, 11%, and 8.9% respectively. As the Na peak in figure 5(d) appears as a single component narrower than those in figure 5(b) and 5(c), one can expect only one kind of Na atom to exist in a (3×1) unit mesh [42]. Considering that the number of atoms of each species in a unit mesh must be an integer, the nearest integer ratio of Na:S'_2:S'_1 is 1:1:2. The differences between the 1:1:2 ratio and the intensity of the fitting results of figure 5(d) are 2% and 7% for S'_1 and S'_2, respectively. Since the (3×1) reconstruction is observed over a wide range of AM coverage, the difference may be due to a small fraction of surface not covered by Na atoms. From these results, it can be deduced that, in a (3×1) unit mesh, there are one Na atom and two kinds of Ge atom of which the relative intensity ratio is 1:2. As a result, the upper limit of the AM coverage is 1/3 ML for the (3×1) surface.

The surface core-level shift (SCLS) results for the (3×1) surfaces of Si and Ge(111) are inconsistent with each other. Paggel *et al* and others reported that the intensity ratio of higher- and lower-binding-energy surface components of the Si 2p core level (S'_1:S'_2) is 1:1 [8, 12, 16]. Zhang *et al* argued that it is 2:1 for Na/Si(111)–3×1 [43]. Göthelid *et al* reported a very different result for K/Ge(111)–3×1 [41]. They reported much larger intensity of the S'_1 component. In our experiment, the intensity ratio is 2:1 (S'_1:S'_2) for the Na/Ge(111)–3×1 surface as shown in figure 5(d). In order to resolve the discrepancies, it is necessary to compare the experimental results with the theoretical calculation of the SCLSs for the proposed models. The calculation must consider many contributing factors such as charge transfer, substrate polarization, covalent bonding character, and the final-state effect [44]. Since no calculations of SCLSs are available at present, we will explain the SCLS results on the basis of the buckled Seiwatz model, which is more favourable as regards the ARPES and total energy calculation results. One reasonable scenario is that S'_1 is associated with two surface Ge atoms just below Na and S'_2 with the π-chained up-Ge atom in the (3×1) unit cell. The other component of the π-chained down-Ge atom is likely to coincide with that of bulk. This is because the charge transfer from the down- to the up-Ge atom in the strongly buckled π-chain can induce such a binding energy separation. The relatively high binding energy of the S'_1 component is probably due to the covalent bonding contribution of Na–Ge bonding in the T_4-site adsorption geometry [44]. In addition, comparing the spectra of figures 5(b) and 5(d), the binding energy of S'_2 is higher and that of Na 2p is lower for the (3×1) surface than those for the RT-deposited surfaces. This indicates that the covalent bonding character of the Na–Ge bonding for the (3×1) surface is larger than that for normal RT-deposited surfaces.

Figure 6 shows the surface E_F-position determined from the bulk Ge 3d position for several Na-adsorbed Ge(111) surfaces. Each $\Delta\phi$ is also plotted as a function of Na coverage. As the Na coverage increases, $\Delta\phi$ decreases, and E_F approaches the valence-band maximum (VBM). As the wafer used is a p-type one, this shift implies that the surface E_F-level moves

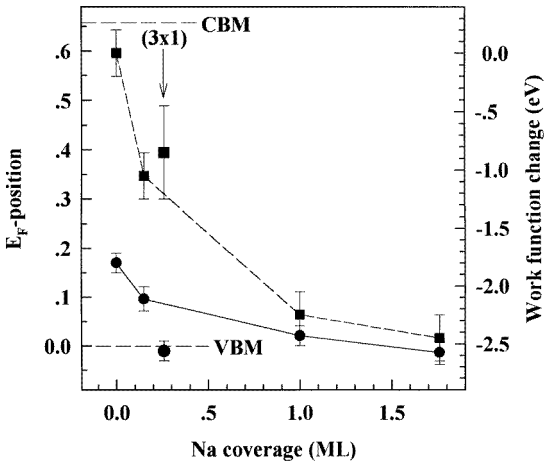

Figure 6. Plots of the surface E_F-position (circles) and work-function change (squares) measured for different surfaces as functions of the Na coverage. The vertical lines are error bars.

to lower energy due to the band-flattening effect after Na deposition. This indicates that the surface charge becomes neutralized with increasing Na coverage, which is in agreement with the previous results [8]. The bulk Ge 3d core level of Na/Ge(111)–3 × 1 is shifted to 0.18 ± 0.01 eV lower binding energy than that of the clean surface. This E_F-position is nearly the same as that of the surface with a thick (1.8 ML) layer of Na, even though the estimated Na coverage is 0.26 ML on the (3 × 1) surface. This band-bending reduction can be understood on the basis of the change of the surface electronic structure influenced by the Na–Ge bonding in the (3 × 1) surface. Since the origin of the band bending of the clean c(2 × 8) surface is the rest-atom state in the band gap, the dramatic change in the structure and bonding in the (3 × 1) surface may decrease a certain partially filled state in the band gap [15] and lead to band flattening. Such an efficient decrement of interfacial gap states is one of the characteristics related to the passivated nature of the (3 × 1) surface. Similarly, the surface Fermi levels of p-type (111) surfaces of Na/Si(111)–3 × 1 [8], B/Si(111)–($\sqrt{3} \times \sqrt{3}$)R30° [24], and K/Ge(111)–3 × 1 [41] are located very close to the respective VBMs, which thus induces a band flattening like in the Na/Ge(111)–3 × 1 case.

4. Conclusion

We investigated the electronic structure of the Na/Ge(111)–3 × 1 surface and discussed its related atomic structure on the basis of the results of valence-band and core-level photoemission spectroscopy. The experimental electronic band structure shows two surface bands in the $\overline{\Gamma}$–$\overline{K}$ and $\overline{\Gamma}$–$\overline{M}$ directions of the SBZ. The band dispersion along $\overline{\Gamma}$–$\overline{K}$ partially agrees with the calculated dispersion for the buckled Seiwatz model. The core-level analysis for Ge 3d reveals that there are two surface components: probably one bonding to Na and another with upward π-chained Ge, respectively. Compared with that of other Na/Ge(111) surfaces, the Na–Ge bonding of the (3 × 1) surface has more covalent character. These changes in atomic and electronic structure of the (3 × 1) surface make the surface E_F pin near the VBM.

Acknowledgments

We thank the UVSOR staff for their assistance during the experiments. We also acknowledge Professor M H Kang for providing unpublished calculation data and Professor D Jeon for helpful discussions. Partial financial support was provided by the Centre for Molecular Science and the Pohang Light Source. One of us (JMS) was supported by the Basic Science Research Institute Programme, Ministry of Education, 1995, Project No BSRI-95-2433.

References

[1] Batra I P 1989 *Metallization and Metal/Semiconductor Interfaces (NATO ASI Series B: Physics, vol 195)* (New York: Plenum)
[2] Daimon H and Ino S 1985 *Surf. Sci.* **164** 320.
[3] Jeon D, Hashizume T, Sakurai T and Willis R F 1992 *Phys. Rev. Lett.* **69** 1419
Jeon D, Hashizume T, Wang X, Bai C, Motai K and Sakurai T 1992 *Japan. J. Appl. Phys.* **31** L501
[4] Tikhov M, Surnev L and Kiskinova M 1991 *Phys. Rev.* B **44** 3222
[5] Weitering H H, DiNardo N J, Pérez-Sandoz R, Chen J and Mele E J 1994 *Phys. Rev.* B **49** 16 839
Carpinelli J M and Weitering H H 1995 *Surf. Sci.* **331/333** 1015
[6] Fan W C and Ignatiev A 1989 *Phys. Rev.* B **40** 5479
Fan W C and Ignatiev A 1990 *Phys. Rev.* B **41** 3592
Fan W C and Ignatiev A 1993 *Surf. Sci.* **296** 352
[7] Hashizume T, Katayama M, Jeon D, Aono M and Sakurai T 1993 *Japan. J. Appl. Phys.* **32** L1263
Jeon D, Hashizume T and Sakurai T 1994 *J. Vac. Sci. Technol.* B **12** 2044
[8] Paggel J J, Haak H, Theis W and Horn K 1993 *J. Vac. Sci. Technol.* B **11** 1439
Paggel J J, Neuhold G, Haak H and Horn K 1995 *Phys. Rev.* B **52** 5813
[9] Sakamoto K, Okuda T, Nishimoto H, Daimon H, Suga S, Kinoshita T and Kakizaki A 1994 *Phys. Rev.* B **50** 1725
[10] Kim J W, Seo J M and Kim S 1996 *Surf. Sci.* **351** L239
[11] Wan K J, Lin X F and Nogami J 1992 *Phys. Rev.* B **46** 13 635
[12] Okuda T, Shigeoka H, Daimon H, Suga S, Kinoshita T and Kakizaki A 1994 *Surf. Sci.* **321** 105
[13] Jeong S and Kang M H 1995 *Phys. Rev.* B **51** 17 635
[14] Erwin S C 1995 *Phys. Rev. Lett.* **75** 1973
[15] Jeong S and Kang M H 1996 *Phys. Rev.* B **54** 8196
[16] Weitering H H, Shi X and Erwin S C 1996 *Phys. Rev.* B **54** 10 585
[17] Jeon D, Hashizume T and Sakurai T 1998 *J. Physique* III **6** C5 189
[18] Pandey K C 1981 *Phys. Rev. Lett.* **47** 1913
Pandey K C 1982 *Phys. Rev. Lett.* **49** 223
[19] Kim J W, Kim S, Seo J M, Tanaka S and Kamada M 1996 *J. Phys.: Condens. Matter* **8** 4189
[20] Yeh J J and Lindau I 1985 *At. Data Nucl. Data Tables* **32** 1
[21] Himpsel F J, Eastman D E, Heimann P, Rheil B, White C W and Zehner D M 1981 *Phys. Rev.* B **24** 1120
Bringans R D and Höchst H 1982 *Phys. Rev.* B **25** 1081
[22] Yokotsuka T, Kono S, Suzuki S and Sagawa T 1984 *J. Phys. Soc. Japan* **53** 696
[23] Takeuchi N, Selloni A and Tosatti E 1992 *Phys. Rev. Lett.* **69** 648
[24] Weitering H H, Chen J, DiNardo N J and Plummer E W 1993 *J. Vac. Sci. Technol.* A **11** 2049
Weitering H H, Chen J, DiNardo N J and Plummer E W 1993 *Phys. Rev.* B **48** 8119
[25] Soukiassian P, Kendelewicz T and Hurych Z D 1989 *Phys. Rev.* B **40** 12 570
[26] Bringans R D, Uhrberg R I G and Bachrach R Z 1986 *Phys. Rev.* B **34** 2373
[27] Wachs A L. Miller T, Hsieh T C, Shapiro A P and Chiang T-C 1985 *Phys. Rev.* B **32** 2326
Chen X H, Ranke W and Schröder-Bergen E 1990 *Phys. Rev.* B **42** 7429
Nicholls J M, Hansson G V, Karlsson U O, Persson P E S, Uhrberg R I G, Engelhardt R, Flodström S A and Koch E-E 1985 *Phys. Rev.* B **32** 6663
[28] Several authors claimed that these are surface resonance features [22, 29], but these peaks also appeared for other metal/Ge systems (Sn/Ge(111)–7×7 [22], Pb/Ge(111)–$(\sqrt{3} \times \sqrt{3})$R30° [30]) since their appearance is not dependent upon the surface structure.
[29] Aarts J, Hoeven A J and Larsen P K 1988 *Phys. Rev.* B **37** 8190
[30] Tonner B P, Li H and Robrecht M J 1987 *Phys. Rev.* B **36** 989

[31] Jeong S and Kang M H, private communication
[32] Nicholls J M, Hansson G V, Karlsson U O, Uhrberg R I G, Engelhardt R, Seki K, Flodström S A and Koch E-E 1984 *Phys. Rev. Lett.* **52** 1555
[33] Joyce J J, Del Giudice M and Weaver J H 1989 *J. Electron Spectrosc. Relat. Phenom.* **49** 31
[34] Schnell R D, Himpsel F J, Bogen A, Rieger D and Steinmann W 1985 *Phys. Rev.* B **32** 8052
Wachs A L, Miller T, Shapiro A P and Chiang T-C 1987 *Phys. Rev.* B **35** 5514
Rich D H, Miller T and Chiang T-C 1988 *Phys. Rev. Lett.* **60** 357
[35] Bringans R D, Olmstead M A, Uhrberg R I G and Bachrach R Z 1987 *Phys. Rev.* B **36** 9569
[36] Takayanagi K and Tanishiro Y 1986 *Phys. Rev.* B **34** 1034
[37] Becker R S, Swartzentruber B S, Vickers J S and Klitsner T 1989 *Phys. Rev.* B **39** 1633
Feenstra R M and Slavin A J 1991 *Surf. Sci.* **251/252** 401
[38] Patthey L, Bullock E L and Hricovini 1992 *Surf. Sci.* **269+270** 28
[39] Göthelid M, Grehk T M, Hammar M, Karlsson U O and Flodström S A 1993 *Phys. Rev.* B **48** 2012
[40] Ma Y, Chen C T, Meigs G, Sette F, Illing G and Shigakawa H 1992 *Phys. Rev.* B **45** 5961
[41] Göthelid M, Odasso S, LeLay G, Björkqvist M, Janin E, Karlsson U O and Grehk T M 1996 *Appl. Surf. Sci.* **104/105** 113
[42] If this 8.9% corresponds to two Na atoms in a (3×1) unit mesh, the total surface atom number in a (3×1) unit mesh becomes 10, which corresponds to 53 surface atoms in the original (2×8) unit mesh. As it is not expected that such a large disruption of the surface resulting in 53 surface atoms in a (2×8) unit mesh, which has 2D surface atoms originally, can be induced by Na evaporation, it is not reasonable to assume that more than one Na atom exists in a (3×1) unit mesh.
[43] Zhang X S, Fan C Y, Xu Y B, Sui H, Bao S, Xu S H, Pan H B and Xu P S 1996 *J. Phys.: Condens. Matter* **8** 699
[44] Clotet A, Ricart J M and Illas F 1996 *Surf. Sci.* **364** 89
Clotet A, Ricart J M, Rubio J and Illas F 1995 *Phys. Rev.* B **51** 1581